Cellular adverse actions of dibromoacetonitrile, a by-product in water bacterial control, at sublethal levels in rat thymocytes

Takumi Kishida[1], Kenji Akiyoshi[2], Erdenebat Erdenedalai[2], Anu Enhetomuru[2], Shoji Imai[1,2], Yasuo Oyama[1,2]

[1] Faculty of Integrated Arts and Sciences, Tokushima University, Tokushima 770-8502, Japan

[2] Graduate School of Integrated Arts and Sciences, Tokushima University, Tokushima 770-8502, Japan

Corresponding author:

Yasuo Oyama, Ph.D.

E-mail: oyamay@tokushima-u.ac.jp

Highlights

• Adverse actions of DBAN at sublethal levels were examined in rat thymocytes.

• DBAN decreased cellular content of nonprotein thiols.

• DBAN increased intracellular Zn^{2+} concentrations by intracellular Zn^{2+} release.

• DBAN at sublethal levels increased cell vulnerability to oxidative stress.

• Environmental risk assessment on DBAN in industrial water may be necessary.

Abstract

The aim of this study was to investigate the effects of dibromoacetonitrile (DBAN), a by-product in water bacterial control, at sublethal concentrations on rat thymocytes, by using a cytometric technique with appropriate fluorescent dyes. By using this method, the possibility that DBAN induces cellular actions related to oxidative stress was assessed. DBAN reduced the content of cellular nonprotein thiols under Zn^{2+}-free conditions. It elevated the intracellular level of Zn^{2+}, being independent from external Zn^{2+}. DBAN increased cell vulnerability to the cytotoxic action of hydrogen peroxide. These actions of DBAN were likely related to oxidative stress. DBAN is formed by the reaction of bromides and chlorinated oxidants during water disinfection. Hydrolysis of 2,2-dibromo-3-nitrilopropionamide, an antimicrobial used in hydraulic fracturing fluids for production of shale gas and oil, produces DBAN. Therefore, the concern regarding the levels of DBAN in industrial water systems is necessary to avoid the environmental risk to humans and wild mammals.

Keywords: dibromoacetonitrile; water disinfection; nonprotein thiol; intracellular Zn^{2+} level; lymphocytes

1. Introduction

With regard to drinking water, the disinfection process is absolutely necessary to avoid waterborne infectious diseases. However, some by-products are generated in the disinfection process (Akin et al., 1982). Some haloacetonitrile by-products have been demonstrated to be hazardous, carcinogenic, mutagenic, genotoxic, and teratogenic under respective experimental conditions (for a review, Yang et al., 2014). The four major species of haloacetonitriles in drinking water are dibromoacetonitrile (DBAN), bromochloroacetonitrile, dichloroacetonitrile, and trichloroacetonitrile (Díaz et al., 2008; Plewa and Wagner, 2008). A previous comparative study using Chinese hamster ovary cells revealed that the toxicities of haloacetonitriles were ordered as follows: DBAN > bromoacetonitrile (BAN) > bromochloroacetonitrile > dichloroacetonitrile > trichloroacetonitrile for cytotoxicity, and BAN = DBAN > bromochloroacetonitrile > trichloroacetonitrile > dichloroacetonitrile for genotoxicity (Muellner et al., 2007). Thus, the bromoacetonitriles (BAN and DBAN) were more toxic than the chloroacetonitriles (dichloroacetonitrile and trichloroacetonitrile). BAN depleted levels of cellular thiols including glutathione (GSH), and induced toxicity (Pals et al., 2016). The *in vivo* applications of DBAN and BAN reduced both superoxide dismutase and glutathione peroxidase activities and increased the level of malonaldehyde in mice (Deng et al., 2017). These results indicated that DBAN and BAN induced oxidative stress. DBAN is also generated by hydrolysis of 2,2-dibromo-3-nitrilopropionamide (DBNPA), an antimicrobial used in hydraulic fracturing fluids (Dow Chemical Company, 2017). It may be more critical because DBNPA, one of major biocides in fracturing fluids, is used in the production of shale gas and oil (Kahrilas et al., 2014; Ferrer and Thurman, 2015). The control of bacteria by antimicrobials including DBAN is necessary to prevent formation of biofilm that disturbs extraction of shale gas and oil.

It was reported that oxidative stress increased intracellular Zn^{2+} concentrations ($[Zn^{2+}]i$) (Slepchenko et al., 2017). Although an excessive increase in $[Zn^{2+}]i$ caused strong oxidative stress (Kanemoto-Kataoka et al., 2017), the cellular content of GSH was increased by the

elevation of $[Zn^{2+}]i$ via intracellular Zn^{2+} release elicited by oxidative or chemical stress (Kinazaki et al., 2011; Fukunaga et al., 2014). Zn^{2+} is an intracellular signal (Hirano et al., 2008). It is a possibility that DBAN and BAN increase oxidative stress, which disturbs intracellular Zn^{2+} homeostasis, resulting in adverse (or lethal) actions. We have tested this possibility by the use of cytometric techniques with fluorescent dyes. This study gives some insights into the diverse actions of bromoacetonitriles.

2. Materials and methods

2.1. Chemicals

DBAN (95% purity) and BAN (99% purity) were obtained from Alfa Aesar (Lancashire, UK) and Tokyo Chemical Industry Co., Ltd. (Tokyo, Japan), respectively. Fluorescent probes and chelators of Zn^{2+} are listed in Table 1. Other chemicals were obtained from Wako Pure Chemicals (Osaka, Japan) unless mentioned otherwise.

(Table 1)

2.2. Animals and cell preparation

The study was approved by Tokushima University, Tokushima, Japan (T29-52). Cell suspension was prepared as described in previous studies (Matsui et al., 2010). Briefly, the thymus glands were excised from Wistar rats (8- to 10-week-old male, Charles River Japan, Shizuoka, Japan) anesthetized with thiopental. Number of animals was 18. The glands were sliced with a razor (FA-10, Feather Safety Razor Co. Ltd., Osaka, Japan) under ice-chilled conditions. Sliced glands were gently dispersed in ice-chilled Tyrode's solution. The solution containing dissociated thymocytes was passed through a mesh (56 μm diameter) to remove tissue residue. The cells were incubated at 36–37°C for 50–60 min to recover membrane potentials before the experiments. Importantly, the suspension contained small amount of zinc that remained during the preparation (Sakanashi et al., 2009).

Various concentrations of DBAN and BAN (3–100 mM initially dissolved in dimethyl

sulfoxide, DMSO) were added to the suspension (1.998 mL per test tube) to achieve final concentrations of 3-100 μM. The cells were treated with DBAN or BAN for 1–3 h at 36–37°C. The incubation time varied with experimental purpose. A total volume of 100 μL cell suspension was sampled to assess cellular parameters. Acquisition of data from 2×10^3 or 2.5×10^3 cells needed 10–15 s. DMSO at 0.3% or less did not change cell viability of rat thymocytes. No fluorescence was recorded from the reagents except for fluorescent probes.

2.3. Cellular parameter measurements

We recorded the fluorescence of cells treated with fluorescent probes with a flow cytometer (CytoACE-150; JASCO, Tokyo, Japan) (Chikahisa et al., 1996). The fluorescence was examined using equipped software (Version 3.06 for CytoACE-150; JASCO, Tokyo, Japan). To assess the change in cell lethality, propidium iodide (PI) was added to the suspensions to achieve a final concentration of 5 μM. PI fluorescence was recorded for 2 min or longer after the dye application. The excitation for PI was 488 nm. The emission was recorded at 600 ± 20 nm. The cells exhibiting PI fluorescence were considered to be dead cells or membrane-comprised cells. 5-CMF-DA was employed to estimate the content of cellular nonprotein thiols, mainly glutathione (Chikahisa et al., 1996). The cells were treated with 500 nM 5-CMF-DA for 30 min prior to the fluorescence measurement. The fluorescence of 5-CMF was recorded from living cells without PI fluorescence. Increase in 5-CMF fluorescence signifies an increase in intracellular thiol content and vice versa. FluoZin-3-AM was applied to monitor the change in $[Zn^{2+}]i$ (Gee et al., 2002). The cells were then incubated with 500 nM FluoZin-3-AM for 60 min before any fluorescence measurements. FluoZin-3 fluorescence was also recorded from living cells without PI fluorescence. Augmentation of FluoZin-3 fluorescence indicates an elevation of $[Zn^{2+}]i$ and vice versa. The excitation wavelength for 5-CMF and FluoZin-3 was 488 nm while their emission was recorded at 530 ± 20 nm.

2.4. Statistical analysis and presentation

Statistical examination was carried out with Tukey's multivariate analysis. P-values <

0.05 were considered statistically significant. Each experimental series was performed thrice, unless stated otherwise.

3. Results

3.1. Increase in cell lethality by DBAN

Treatment of cells with DBAN at 3–50 μM for 3 h did not cause changes in the histogram of PI fluorescence (Fig. 1A). Thus, DBAN administration at 50 μM or less did not change the percentage of dead cells or membrane-comprised cells in the population (Fig. 1B). However, cell treatment with 100 μM DBAN for 3 h significantly increased the population of cells that demonstrated PI fluorescence (Fig. 1A), indicating a significant increase in cell lethality (Fig. 1B). The application of 100 μM BAN for 3 h did not affect the population of cells with PI fluorescence (not shown). Therefore, further experiments on BAN were not carried out.

(Figure 1)

3.2. Changes in forward and side scatter by DBAN

A large population of cells was dead when the cells were treated with 100 μM DBAN for 3 h. The cell death induced by 100 μM DBAN was associated with decreased intensities of forward and side scatter (Fig. 2A and 2B), indicating shrunken dead cells. Treatment with DBAN at 50 μM, a sublethal concentration, for 3 h slightly increased the intensity of side scatter but did not change the intensity of forward scatter in thymocytes (Fig. 2B). Thus, DBAN at 50 μM increased cell density (or cell granularity) that reflected changes in intracellular circumstance.

(Figure 2)

3.3. Changes in the cellular content of nonprotein thiols by DBAN

The treatment of thymocytes with 30 μM DBAN for 1.5 h increased the intensity of 5-CMF fluorescence, resulting in a shift of the histogram of PI fluorescence to the direction of higher intensity (Fig. 3A). The concentration-response relationship for DBAN-induced changes

in 5-CMF fluorescence is shown in Fig. 3B. The relationship was bell-shaped with the peak intensity of 5-CMF fluorescence recorded from the cells treated with 30 μM DBAN. The treatment with 100 μM DBAN for 1.5 h greatly attenuated 5-CMF fluorescence recorded only from living cells that were not stained with propidium. Thus, DBAN at concentrations of 30 μM and 100 μM were supposed to increase and decrease the cellular content of nonprotein thiols, respectively.

(Figure 3)

3.4. Elevation in $[Zn^{2+}]i$ by DBAN

Converting thiols to disulfide linkages induces intracellular Zn^{2+} release, resulting in an increase in $[Zn^{2+}]i$, because thiols form complexes with Zn^{2+}. As shown in Fig. 4A, the treatment of thymocytes with 30–50 μM DBAN for 1.5 h shifted the histogram of FluoZin-3 fluorescence to a region of higher intensity, indicating the DBAN-induced elevation of $[Zn^{2+}]i$. The concentration-response relationship is shown in Fig. 4B. DBAN at concentrations of 30–50 μM similarly increased the intensity of FluoZin-3 fluorescence in the presence of DTPA, which chelated extracellular Zn^{2+} (Fig. 5). DBAN at 30–50 μM failed to augment FluoZin-3 fluorescence in the presence of TPEN.

(Figures 4 and 5)

3.5. Effect of TPEN on DBAN-induced changes in cellular content of nonprotein thiols

DBAN at a concentration of 30 μM failed to augment 5-CMF fluorescence in the presence of TPEN that chelated intracellular Zn^{2+}. Furthermore, DBAN at a concentration of 50 μM further reduced the intensity of FluoZin-3 fluorescence. It is likely that the increase in cellular content of nonprotein thiols by DBAN is Zn^{2+}-dependent.

(Figure 6)

3.6. Effect of DBAN on cell vulnerability to oxidative stress

Changes in the cellular content of nonprotein thiols and $[Zn^{2+}]i$ are linked to cellular redox. The treatment with 300 μM H_2O_2 to induce oxidative stress for 3 h increased cell

lethality to 10%–20% while it was about 5% under control conditions. DBAN at sublethal levels (30–50 μM) further increased the lethality of cells simultaneously treated with 300 μM H_2O_2 (Fig. 7).

(Figure 7)

4. Discussion

DBAN at sublethal concentrations (3–50 μM) exhibited a bell-shaped relationship with respect to the change in the cellular content of nonprotein thiols (Fig. 3B). DBAN at 30 μM increased the cellular content, while it was decreased under intracellular Zn^{2+}-free conditions manipulated with TPEN (Fig. 3B and 6). Thus, the increase induced by 30 μM DBAN is considered to be Zn^{2+}-dependent. Under intracellular Zn^{2+}-free conditions, DBAN at 50 μM significantly reduced the cellular content of nonprotein thiols. Therefore, it is hypothesized that DBAN induces oxidative stress, resulting in the reduction of nonprotein thiol content. Oxidative stress converts thiols to disulfides, resulting in the release of Zn^{2+} (Maret, 2009). DBAN at 3–50 μM elevated $[Zn^{2+}]i$ in a concentration-dependent manner (Fig. 4B). The elevation in $[Zn^{2+}]i$ by DBAN was similarly observed under extracellular Zn^{2+}-free conditions manipulated with DTPA (Fig. 5). Thus, this increase was due to the DBAN-induced release of intracellular Zn^{2+}. These observations support the hypothesis described above. The treatment of cells with H_2O_2 decreased cellular thiol content and increased $[Zn^{2+}]i$ (Chikahisa et al., 1996; Matsui et al., 2010). An excessive increase in $[Zn^{2+}]i$ induced oxidative stress (Oyama et al., 2012; Slepchenko et al., 2017). Therefore, it is plausible to predict that DBAN increases cell vulnerability to oxidative stress induced by H_2O_2. In fact, simultaneous application of 30–50 μM DBAN and 300 μM H_2O_2 produced a further increase to cell lethality (Fig. 7). In conclusion, DBAN, even at sublethal concentrations, exerts oxidative stress in mammalian cells.

DBAN is formed during disinfection as a result of the reaction of bromides with chlorinated oxidizing compounds (Huang et al., 2003). Drinking water in developed countries

contains small amounts of DBAN (International Agency for Research on Cancer, 2013); however, this is lower than the concentration that induced cellular actions under *in vitro* conditions. Thus, it is not considered that DBAN in drinking water elicits adverse cellular actions. However, some amounts of DBAN may be present in industrial systems because hydrolysis of DBNPA, an antimicrobial compound, produces DBAN (Dow Chemical Company, 2017). DBNPA is used to treat various processing and recycle water systems in many industrial fields. Thus, the content of DBAN in hydraulic fracturing fluids for the production of shale gas and oil should be concerned although the cytotoxicity of DBAN, described in this study, is lower than that of DBNPA (Ishikawa et al., 2016).

Conflict of interest

All authors declare no conflicts of interest.

Acknowledgements

This study was supported by Grant-in-Aids for Scientific Research (C26340039) awarded to Y. Oyama from the Japan Society for the Promotion of Science (Tokyo, Japan).

References

Akin, E.W., Hoff, J.C., Lippy, E.C., 1982. Waterborne outbreak control: Which disinfectant? Environ. Health Perspect. 46, 7–12.

Chikahisa, L., Oyama, Y., Okazaki, E., Noda, K., 1996. Fluorescent estimation of H_2O_2-induced changes in cell viability and cellular nonprotein thiol level of dissociated rat thymocytes. Jpn. J. Pharmacol. 71, 299–305.

Deng, Y., Zhang, Y., Lu, Y., Lu, K., Bai, H., Ren, H., 2017. Metabolomics evaluation of the in vivo toxicity of bromoacetonitriles: One class of high-risk nitrogenous disinfection byproducts. Sci. Total Environ. 579, 107-114.

Díaz, F.J., Chow, A.T., O′Geen, A.T., Dahlgren, R.A., Wong, P.K., 2008. Restored wetlands as a source of disinfection byproduct precursors. Environ. Sci. Technol. 42, 5992–5997.

Dow Chemical Company, Dow Answer Center, 2017. What can you tell me about decomposition in DOWICIL™ QK-20 antimicrobial products? https://dowac.custhelp.com/app/answers/detail/a_id/2331/~/dowicil-qk-20-decomposition-pathways

Ferrer, I. Thurman, E.M., 2015. Chemical constituents and analytical approaches for hydraulic fracturing waters. Trend Environ. Anal. Chem. 5, 18–25.

Fukunaga, E., Ishida, S., Oyama, Y., 2014. Changes in cellular thiol content and intracellular Zn^{2+} level by 1,4-naphthoquinone in rat thymocytes. Chem. Biol. Interact. 222, 1–6.

Gee, K.R., Zhou, Z.L., Qian, W.J., Kennedy, R., 2002. Detection and imaging of zinc secretion from pancreatic β-cells using a new fluorescent zinc indicator. J. Amer. Chem. Soc. 124, 776–778.

Hirano, T., Murakami, M., Fukada, T., Nishida, K., Yamasaki, S., Suzuki, T., 2008. Roles of zinc and zinc signaling in immunity: zinc as an intracellular signaling molecule. Adv. Immunol. 97, 149–176.

Huang, W.J., Tsai, Y.Y., Chu, C., 2003. Evaluation of disinfection by-products formation

during ozonation of bromide-containing groundwater. J. Environ. Sci. Health Part A. 38, 2919–2931.

Ishikawa, M., Muraguchi, R., Azuma, A., Nawata, S., Miya, M., Katsuura, T., .Naito, T., Oyama, Y., 2016. Cytotoxic actions of 2, 2-dibromo-3-nitrilopropionamide, a biocide in hydraulic fracturing fluids, on rat thymocytes. Toxicol. Rese. 5, 1329–1334.

International Agency for Research on Cancer, IARC Working Group on the Evaluation of Carcinogenic Risks to Humans, 2013. Some chemicals present in industrial and consumer products, food and drinking-water. IARC monographs on the evaluation of carcinogenic risks to humans. 101, 533–550.

Kahrilas, G.A., Blotevogel, J., Stewart, P.S., Borch, T., 2014. Biocides in hydraulic fracturing fluids: A critical review of their usage, mobility, degradation, and toxicity. Environ. Sci. Technol. 49, 16–32.

Kanemoto-Kataoka, Y., Oyama, T.M., Ishibashi, H., Oyama, Y., 2017. Zinc is a determinant of the cytotoxicity of Ziram, a dithiocarbamate fungicide, in rat thymic lymphocytes: possible environmental risks. Toxicol. Res. 6, 499–504.

Kinazaki, A., Chen, H., Koizumi, K., Kawanai, T., Oyama, T.M., Satoh, M., Ishida, S., Okano, Y., Oyama, Y., 2011. Putative role of intracellular Zn^{2+} release during oxidative stress: a trigger to restore cellular thiol content that is decreased by oxidative stress. J. Physiol. Sci. 61, 403–409.

Maret, W., 1994. Oxidative metal release from metallothionein via zinc-thiol/disulfide interchange. Proc. Natl. Acad. Sci. U.S.A. 91, 237–241.

Matsui, H., Oyama, T.M., Okano, Y., Hashimoto, E., Kawanai, T., Oyama, Y., 2010. Low micromolar zinc exerts cytotoxic action under H_2O_2-induced oxidative stress: Excessive increase in intracellular Zn^{2+} concentration. Toxicology. 276, 27–32.

Muellner, M.G., Wagner, E.D., McCalla, K., Richardson, S.D., Woo, Y.T., Plewa, M.J., 2007. Haloacetonitriles vs. regulated haloacetic acids: Are nitrogen-containing DBPs more toxic?

Environ. Sci. Technol. 41, 645–651.

Oyama, T.M., Saito, M., Yonezawa, T., Okano, Y., Oyama, Y., 2012. Nanomolar concentrations of zinc pyrithione increase cell susceptibility to oxidative stress induced by hydrogen peroxide in rat thymocytes. Chemosphere. 87, 1316–1322.

Pals, J.A., Ang, J.K., Wagner, E.D., Plewa, M.J., 2011. Biological mechanism for the toxicity of haloacetic acid drinking water disinfection byproducts. Environ. Sci. Technol. 45, 5791–5797.

Plewa, M.J., Wagner, E.D., 2008. Emerging Health Concerns Related to Water Treatment. Illinois State Water Survey, Midwest Technology Assistance Center for Small Public Water Systems (MTAC). http://mtac.isws.illinois.edu/mtacdocs/pubs/MTACTR08-05.pdf

Sakanashi, Y., Oyama, T.M., Matsuo, Y., Oyama, T.B., Nishimura, Y., Ishida, S., Imai, S., Okano, Y., Oyama, Y., 2009. Zn^{2+}, derived from cell preparation, partly attenuates Ca^{2+}-dependent cell death induced by A23187, calcium ionophore, in rat thymocytes. Toxicology In Vitro. 23, 338–345.

Slepchenko, K.G., Lu, Q., Li, Y.V., 2017. Cross talk between increased intracellular zinc (Zn^{2+}) and accumulation of reactive oxygen species in chemical ischemia. Am. J. Physiol.-Cell Physiol. 313, C448–C459.

Yu, Y., Wei, X., Zhang, X., 2014. Formation and toxicity of haloacetonitriles in drinking water: a review of recent studies. J. Environ. Health, 8, 32.

Legends

Figure 1. DBAN-induced increase in cells exhibiting PI fluorescence (cell lethality). (A) Histograms of PI fluorescence recorded from cells treated with DBAN. Each histogram was constructed using 2500 cells. Cytogram is a representative one in eighteen measurements. (B) Concentration-response relationship for DBAN-induced changes in cell lethality. Columns and bars show mean ± standard deviation of six to eight samples. Each experimental series was performed thrice. Asterisks (**) indicate significant differences ($P < 0.01$) between the control group (CONTROL) and the group of cells treated with DBAN.

Figure 2. DBAN-induced change in forward and side scatter. (A) Cytogram of cells treated with 100 μM DBAN. Cytogram was constructed using 2500 cells. Cytogram is a representative one in eighteen measurements. The intensity of forward scatter, light diffraction around one cell, is proportional to the diameter of the cell. The forward scatter measurement can discriminate the cells by size. The measurement of side scatter that is caused by the interface between the laser and intracellular structures shows the internal complexity of a cell. (B) DBAN-induced changes in forward and side scatter. Columns and bars show mean ± standard deviation of four samples. Each experimental series was performed thrice. Asterisks (**) indicate significant differences ($P < 0.01$) between the control group (CONTROL) and the group of cells treated with DBAN.

Figure 3. DBAN-induced change in 5-CMF fluorescence. (A) Histograms of 5-CMF fluorescence recorded from living cells treated with DBAN. Each histogram was constructed using 2500 cells. Histogram is a representative one in twelve measurements. (B) Concentration-response relationship for DBAN-induced change in mean intensity of 5-CMF fluorescence. Columns and bars show mean ± standard deviation of four samples. Each experimental series was performed thrice. Asterisks (**) indicate significant differences ($P < 0.01$) between the

control group (CONTROL) and the group of cells treated with DBAN.

Figure 4. DBAN-induced increase in FluoZin-3 fluorescence. (A) Histograms of FluoZin-3 fluorescence recorded from living cells treated with DBAN. Each histogram was constructed using 2500 cells. Histogram is a representative one in twelve measurements. (B) Concentration-response relationship for DBAN-induced change in mean intensity of FluoZin-3 fluorescence. Columns and bars show mean ± standard deviation of four samples. Each experimental series was performed thrice. Asterisks (**) indicate significant differences ($P < 0.01$) between the control group (CONTROL) and the group of cells treated with DBAN.

Figure 5. DBAN-induced change in mean intensity of FluoZin-3 fluorescence under Zn^{2+}-free conditions prepared with DTPA or TPEN, respectively. Columns and bars show mean ± standard deviation of four samples. Each experimental series was performed twice. Asterisks (**) indicate significant differences ($P < 0.01$) between the control group (CONTROL) and the group of cells treated with DBAN.

Figure 6. DBAN-induced change in mean intensity of 5-CMF fluorescence under Zn^{2+}-free condition prepared with TPEN. Columns and bars show mean ± standard deviation of four samples. Each experimental series was performed thrice. Asterisks (**) indicate significant differences ($P < 0.01$) between the control group (CONTROL) and the group of cells treated with DBAN.

Figure 7. DBAN-induced increase in cell vulnerability due to H_2O_2-induced oxidative stress . Columns and bars show mean ± standard deviation of cell lethality (percentage population of cells exhibiting PI fluorescence) in four samples. Each experimental series was performed thrice. Asterisks (**) indicate significant differences ($P < 0.01$) between the control group

(CONTROL) and the group of cells treated with DBAN, H_2O_2, or both. Pounds (##) show significant differences ($P < 0.01$) between the control group (CONTROL) and the group of cells treated with DBAN in the presence of H_2O_2.

Table 1. Specific reagents used in this study

A. Fluorescent probes [Manufacturer]	Emission Wavelength
Propidium Iodide (PI) [Molecular Probes, Inc., Eugene, OR, USA]	PI: 600 ± 20 nm
FluoZin-3-AM [Molecular Probes]	FluoZin-3: 530 ± 20 nm
5-Chloromethylfluorescein Diacetate (5-CMF-DA) [Molecular Probes]	5-CMF: 530 ± 20 nm

(*) Excitation wavelength was 488 nm for all fluorescent probes.

B. Zinc chelator [Manufacturer]	Purpose
Diethylenetriamine-N,N,N′,N″,N″-pentaacetic acid (DTPA) [Dojin Chemical Laboratory, Kumamoto, Japan]	Chelating external Zn^{2+}
N,N,N′,N′-tetrakis(2-pyridylmethyl)ethylenediamine (TPEN) [Dojin Chemical Laboratory]	Chelating intracellular Zn^{2+}

Figure 1

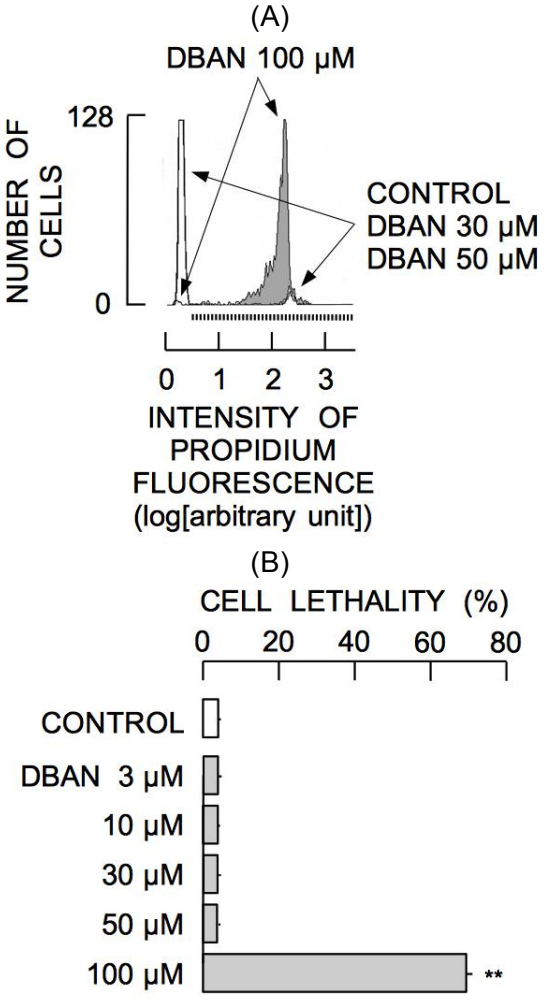
(A)
DBAN 100 μM
128
0
NUMBER OF CELLS
CONTROL
DBAN 30 μM
DBAN 50 μM
0 1 2 3
INTENSITY OF PROPIDIUM FLUORESCENCE
(log[arbitrary unit])
(B)
CELL LETHALITY (%)
0 20 40 60 80
CONTROL
DBAN 3 μM
10 μM
30 μM
50 μM
100 μM
**

Figure 2

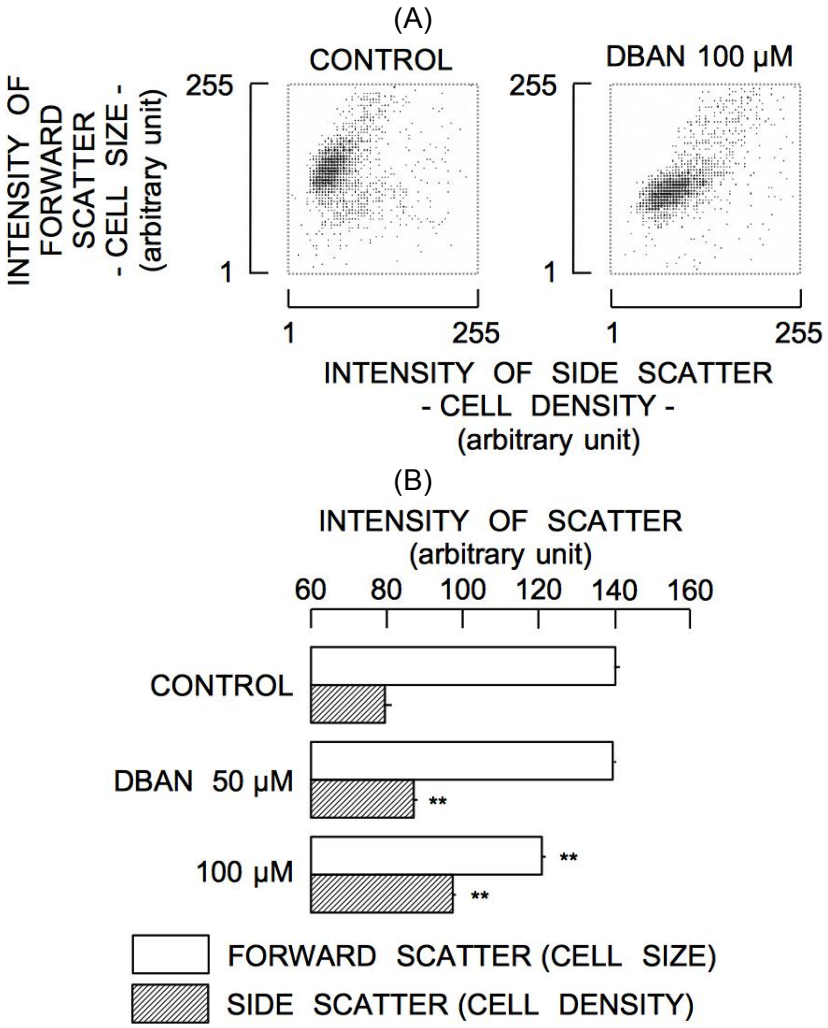
(A)
CONTROL
DBAN 100 μM
INTENSITY OF FORWARD SCATTER - CELL SIZE - (arbitrary unit)
255
1
1
255
INTENSITY OF SIDE SCATTER - CELL DENSITY - (arbitrary unit)
(B)
INTENSITY OF SCATTER (arbitrary unit)
60 80 100 120 140 160
CONTROL
DBAN 50 μM
100 μM
**
FORWARD SCATTER (CELL SIZE)
SIDE SCATTER (CELL DENSITY)

Figure 3

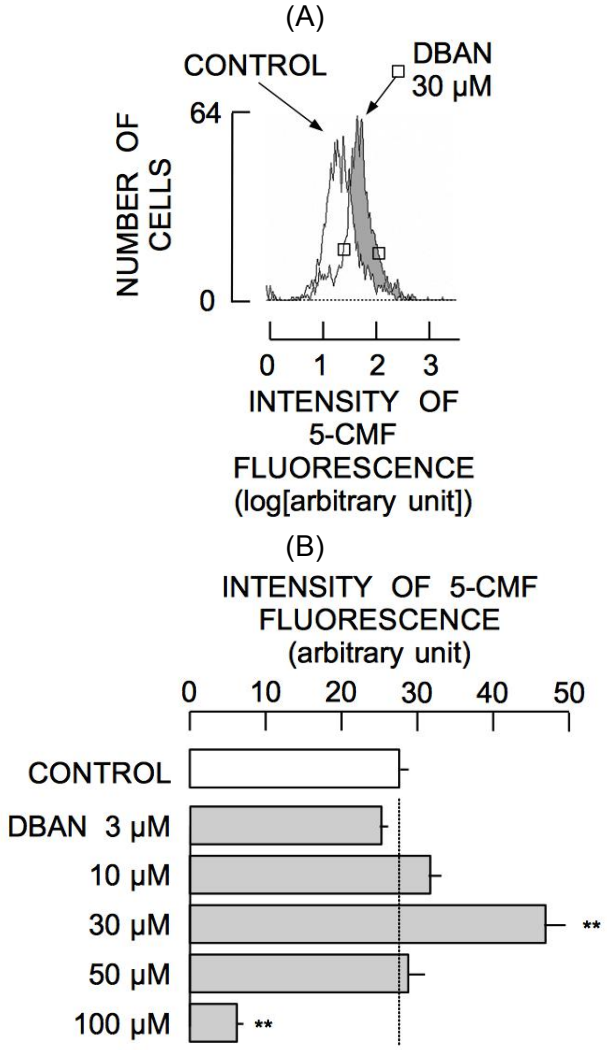
(A)
CONTROL
DBAN
30 μM
64
0
NUMBER OF CELLS
0 1 2 3
INTENSITY OF 5-CMF FLUORESCENCE (log[arbitrary unit])
(B)
INTENSITY OF 5-CMF FLUORESCENCE (arbitrary unit)
0 10 20 30 40 50
CONTROL
DBAN 3 μM
10 μM
30 μM
50 μM
100 μM
**
**

Figure 4

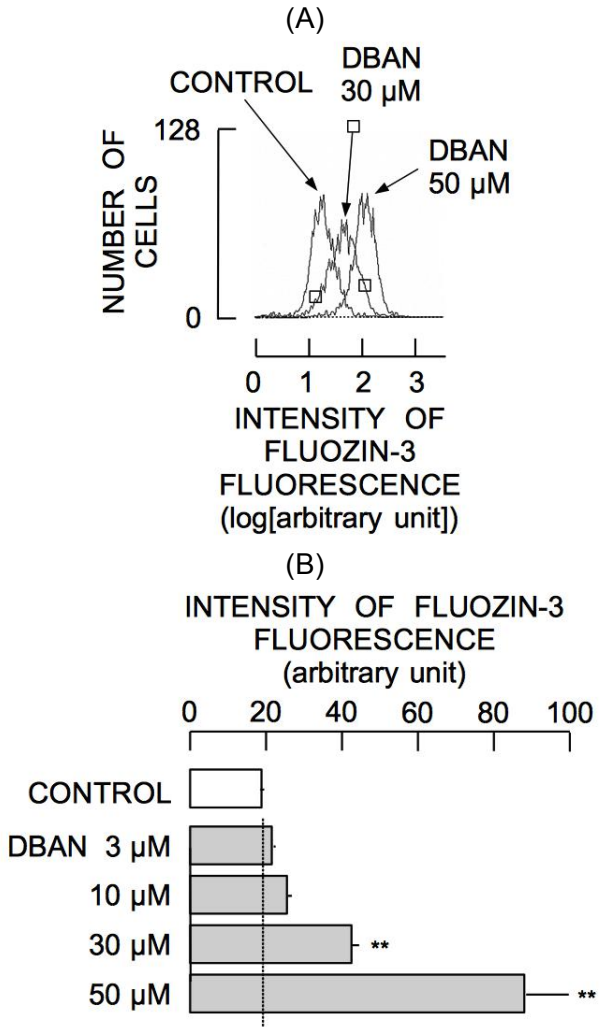
(A)
CONTROL
DBAN
30 μM
DBAN
50 μM
128
0
NUMBER OF CELLS
0 1 2 3
INTENSITY OF FLUOZIN-3 FLUORESCENCE
(log[arbitrary unit])
(B)
INTENSITY OF FLUOZIN-3 FLUORESCENCE
(arbitrary unit)
0 20 40 60 80 100
CONTROL
DBAN 3 μM
10 μM
30 μM
50 μM
**
**

Figure 5

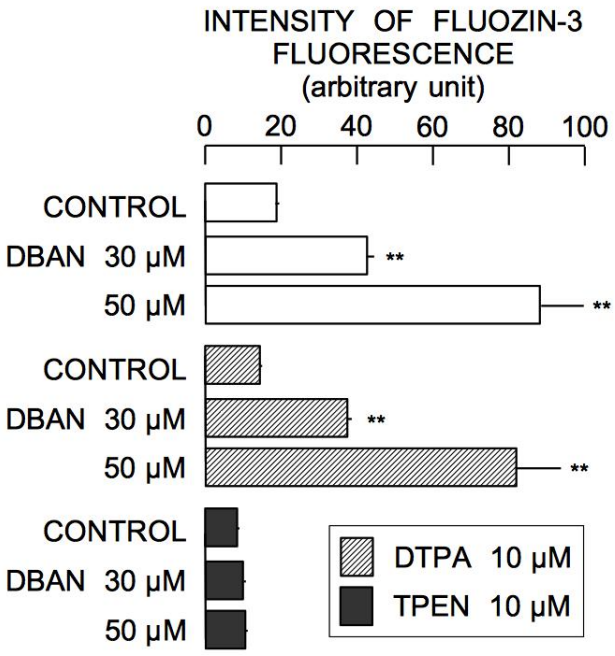
INTENSITY OF FLUOZIN-3 FLUORESCENCE
(arbitrary unit)
0
20
40
60
80
100
CONTROL
DBAN 30 μM
50 μM
**
**
CONTROL
DBAN 30 μM
50 μM
**
**
CONTROL
DBAN 30 μM
50 μM
DTPA 10 μM
TPEN 10 μM

Figure 6

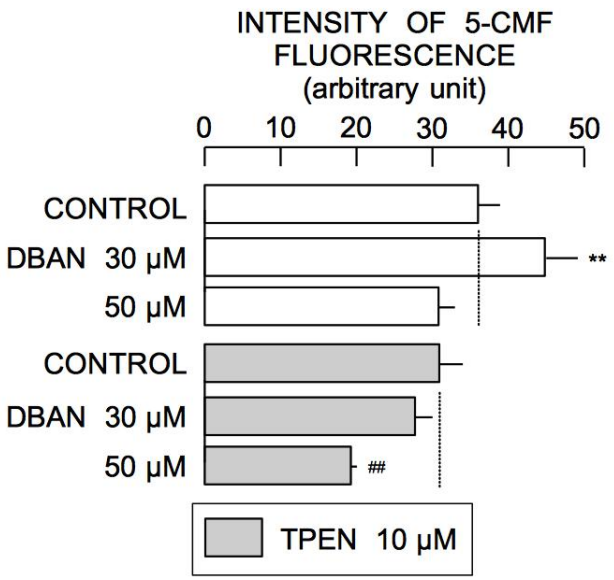
INTENSITY OF 5-CMF
FLUORESCENCE
(arbitrary unit)
0
10
20
30
40
50
CONTROL
DBAN 30 μM
50 μM
**
CONTROL
DBAN 30 μM
50 μM
##
TPEN 10 μM

Figure 7

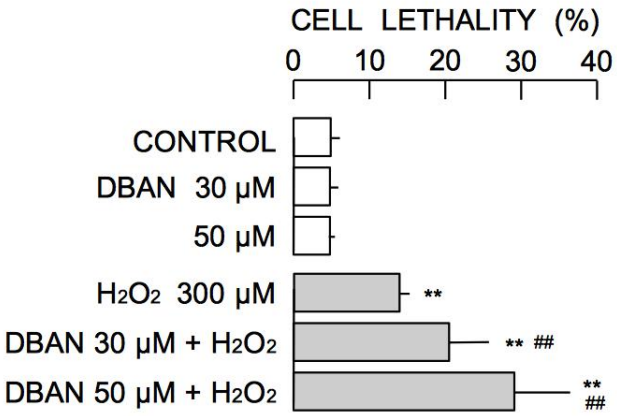
CELL LETHALITY (%)
0
10
20
30
40
CONTROL
DBAN 30 μM
50 μM
H2O2 300 μM
DBAN 30 μM + H2O2
DBAN 50 μM + H2O2
**
** ##
** ##